

CORONAL MASS EJECTION INITIATION: ON THE NATURE OF THE FLUX CANCELLATION MODEL

T. AMARI^{1,2,3,4}, J.-J. ALY², Z. MIKIC³, AND J. LINKER³

¹ CNRS, Centre de Physique Théorique de l'École Polytechnique, F-91128 Palaiseau Cedex, France; amari@cpht.polytechnique.fr

² AIM, Unité Mixte de Recherche CEA, CNRS, Université Paris VII, UMR n° 7158, Centre d'Études de Saclay, F-91191 Gif sur Yvette Cedex, France

³ Predictive Science Inc., San Diego, CA 92121, USA

Received 2010 February 20; accepted 2010 May 10; published 2010 June 10

ABSTRACT

We consider a three-dimensional bipolar force-free magnetic field with a nonzero magnetic helicity, occupying a half-space, and study the problem of its evolution driven by an imposed photospheric flux decrease. For this specific setting of the Flux Cancellation Model describing coronal mass ejections occurring in active regions, we address the issues of the physical meaning of flux decrease, of the influence on field evolution of the size of the domain over which this decrease is imposed, and of the existence of an energetic criterion characterizing the possible onset of disruption of the configuration. We show that (1) the imposed flux disappearance can be interpreted in terms of transport of positive and negative fluxes toward the inversion line, where they get annihilated. (2) For the particular case actually computed, in which the initial state is quite sheared, the formation of a twisted flux rope and the subsequent global disruption of the configuration are obtained when the flux has decreased by only a modest amount over a limited part of the whole active region. (3) The disruption is produced when the magnetic energy becomes of the order of the decreasing energy of a semi-open field, and then before reaching the energy of the associated fully open field. This suggests that the mechanism leading to the disruption is nonequilibrium as in the case where flux is imposed to decrease over the whole region.

Key words: magnetohydrodynamics (MHD) – stars: coronae – stars: flare – stars: magnetic field – Sun: coronal mass ejections (CMEs) – Sun: flares

Online-only material: color figures

1. INTRODUCTION

Magnetic flux cancellation (FC) is a well-documented solar photospheric phenomenon (Welsch 2006) which plays the key role in the Flux Cancellation Model (FCM). The FCM has been introduced initially to explain flux rope and prominence formation (van Ballegooyen & Martens 1989) and applied later on for modeling large-scale eruptive events such as coronal mass ejections (CMEs) occurring in active regions (see, e.g., Forbes et al. 2006 for a review). In the latter context, it has been actually developed in two settings differing from each other essentially by the way FC is introduced: FC is either taken to be a physical consequence of the photospheric turbulent diffusion, or just imposed as a time-dependent boundary condition describing a decrease of the flux according to some prescribed law. In the former case, first considered in Amari et al. (2003b) and later on in Yeates & Mackay (2009), Yeates et al. (2010), and Aulanier et al. (2010), the dispersive effect of the turbulence on the flux of an active region leads to the bringing together on the inversion line of some amount of flux of both polarities, which thus gets annihilated by small-scale mixing. This type of FCM is of course particularly relevant when one wants to explain the CMEs that occur during the decaying phase of an active region. The second type of FC implementation was first applied to study the possible disruption of two-dimensional bipolar configurations (Forbes & Priest 1995) and later on of three-dimensional bipolar configurations (Amari et al. 2000; Linker et al. 2001) and three-dimensional quadrupolar ones (Amari et al. 2007).

Although previous works have led to a good understanding of the FCM in the “flux decreasing setting,” there are many

points which are still unclear. (1) The disappearance of flux on the boundary is imposed as a mere mathematical boundary condition, and doubts have been sometimes expressed about the possibility that it is related to some physical process. To keep this setting of the FCM viable, we thus need to provide a physical interpretation of flux decrease that is compatible with the observations. For instance, the latter show FC to be often associated with the mutual annihilation of opposite polarity flux elements brought into contact by photospheric motions, and an interpretation in terms of flux transport and annihilation on an inversion line would be certainly adequate. Another possibility would be to interpret FC in terms of emergence through the photosphere of either a U-loop or a bipolar loop, with flux decrease occurring in the latter case once the magnetic axis has started emerging (see Fan 2001 and Amari et al. 2005 for simulations, and López Fuentes et al. 2000 for observations). (2) Previously, flux decrease has been imposed to occur over the whole active region, or at least the whole central bipolar part in the case of a quadrupolar region (Amari et al. 2007). In many cases, however, one may expect FC to occur over only a small part of the region, and the question arises of the possibility of still triggering a disruption in that case. (3) If a disruption actually occurs, we finally have to address the question of the nature of its trigger. Basically, there are three possible mechanisms (Amari & Aly 2009): nonequilibrium (NE), quasi-nonequilibrium (QNE), meaning equilibrium too far to be accessible, and unstable equilibrium (UE). For instance, we found QNE to be responsible for the transition to very fast expansion exhibited by a flux rope twisted by boundary motions (Amari et al. 1996). In the case of a bipolar (Amari et al. 2000) or quadrupolar (Amari et al. 2007) configuration submitted to FC, on the contrary, we found NE to be at the origin of the eruption. This conclusion was established by showing that the magnetic energy of the system exceeds the

⁴ Also associate scientist at Observatoire de Paris, LESIA, 5 place Jules Janssen, F-92190 Meudon Cedex, France.

energy of the associated totally open field in the former case, and the energy of a partially open field (having its open lines being connected only to the part of the boundary where strong currents once developed) in the latter one. Then we should look in particular for the existence of a similar energy criterion if a disruption occurs as a consequence of partial FC.

The aim of this Letter is to address these important issues in the case where the initial configuration is force free and has a nonzero magnetic helicity. Physically, such a field may be thought of as either resulting from the emergence of a twisted flux rope (TFR) through the photosphere, or being the remnant of a configuration which has previously generated an eruptive event without fully relaxing to a potential field (Amari & Luciani 1999), or being produced by photospheric twisting motions. It is worth insisting on the fact that the evolutions we consider are only driven by FC, in opposition to some other works (van Ballegooijen et al. 2000; Aulanier et al. 2010) in which FC is applied along with shearing motions.

2. MODEL AND INITIAL CONFIGURATION

In our numerical model, the “coronal half-space” $\{z > 0\}$ above an active region is represented by a large computational box $\Omega_h = [-20, 20] \times [-20, 20] \times [0, 40]$, equipped with a nonuniform mesh of $141 \times 131 \times 121$ nodes. The physical quantities used are dimensionless. In particular, the Alfvén crossing time τ_A is taken as the time unit. Ω_h contains a perfectly conducting low-density plasma with an embedded magnetic field \mathbf{B} . For $t \geq 0$, this system is brought into a two-stage magnetohydrodynamics (MHD) evolution: a preliminary stage, not claimed to represent an actual coronal evolution, which produces a force-free equilibrium with a nonzero helicity, and a second stage, which is the physically relevant one, in which the previous field is taken as the initial state of an FC-driven evolution. Both phases are controlled by imposing on the “photospheric” boundary S_h of Ω_h (on which $z = 0$) the tangential component of the electric field, \mathbf{E}_s , a procedure which is known from our previous works to lead to a well-posed problem. Quite generally, \mathbf{E}_s can be Helmholtz decomposed according to

$$c \mathbf{E}_s = \nabla_s \phi + \nabla_s \psi \times \hat{\mathbf{z}}, \quad (1)$$

where $\nabla_s = \hat{\mathbf{x}} \partial_x + \hat{\mathbf{y}} \partial_y$, and $\phi(x, y, t)$ and $\psi(x, y, t)$ are solutions, respectively, of the equations $\nabla_s^2 \phi = c \nabla_s \cdot \mathbf{E}_s$ and $-\nabla_s^2 \psi = c \hat{\mathbf{z}} \cdot \nabla_s \times \mathbf{E}_s$. Using Faraday law thus leads to

$$\partial_t B_z = -c \nabla \cdot (\mathbf{E}_s \times \hat{\mathbf{z}}) = \nabla_s^2 \psi. \quad (2)$$

The MHD equations are solved by our numerical algorithm (Amari et al. 1999, 1996). Small values are chosen for the dissipation coefficients: $\nu = 10^{-2}$ – 10^{-3} for the kinematic viscosity, and η not larger than 10^{-4} for the resistivity, giving for our mesh resolution a Lundquist number not smaller than 10^4 .

In the first stage, we start at $t = 0$ from a bipolar potential magnetic field $\mathbf{B}_\pi = \nabla V_\pi$. V_π is the solution of a Dirichlet–Neuman boundary value problem for the Laplace equation, in which we impose in particular the condition

$$B_{\pi z}(x, y, 0) = q(x, y) = e^{-x^2/\sigma_x^2} \times (e^{-(y-y_c)^2/\sigma_y^2} - e^{-(y+y_c)^2/\sigma_y^2}) \quad (3)$$

on S_h , with $y_c = -0.8$, $\sigma_x = 1$, $\sigma_y = 2$. For $0 \leq t \leq 400$, we apply on S_h , as in Amari et al. (2003a), the tangential electric

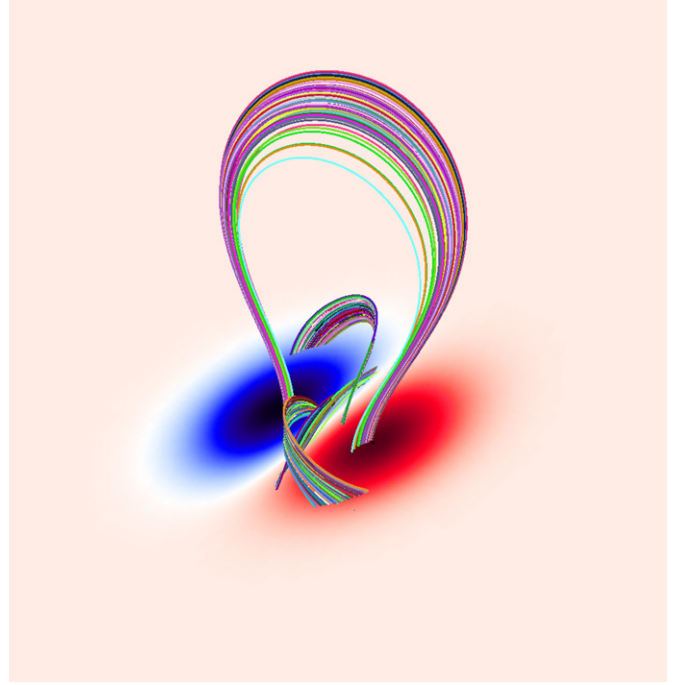


Figure 1. Selected field lines of the initial force-free configuration reached after a shearing–twisting phase followed by a viscous relaxation. Strong shear is accumulated along the neutral line.

(A color version of this figure is available in the online journal.)

field \mathbf{E}_s associated with $\psi = 0$ and a ϕ such that $\phi'(B_z) = B_z \Phi'(B_z)$, with $\Phi(B_z)$ being a prescribed function. This generates slow shearing/twisting B_z -preserving ideal motions of the magnetic footpoints at the velocity $\mathbf{v}_s = c \nabla_s \phi \times \hat{\mathbf{z}} B_z$ (with $\max(v_s) = 10^{-2}$). A neighboring nonlinear force-free equilibrium is next reached by performing for $400 \leq t \leq 800 = t_0$ a viscous relaxation phase during which $\phi = \psi = 0$ and B_z is still conserved on S_h . As shown in Figure 1, this equilibrium is sheared along the neutral line, and because of twist, it exhibits away from that line the presence of strong electric currents correlated with the typical sigmoidal structure. It is worth noting that, for this equilibrium, we have $\text{supp}(\text{FFF}) \subset \text{supp}(B_z)$, where $\text{supp}(\text{FFF})$ and $\text{supp}(B_z)$ denote the regions where, respectively, electric currents and B_z are strong enough.

3. PARTIAL FLUX CANCELLATION

For driving the FC phase, we fix \mathbf{E}_s on S_h by setting $\phi(x, y, t) = 0$ and by taking ψ to satisfy $\nabla_s^2 \psi(x, y, t) = -\mu \zeta(y) B_z(x, y, 0, t_0) = -\mu \zeta(y) q(x, y)$ on S_h , with $\mu = 10^{-2} > 0$, and $\zeta(y) = (1 + \tanh((y_1 - y)/d))(1 + \tanh((y - y_0)/d))/4$. ζ exhibits a “plateau” of height 1 in the interval $[y_0, y_1]$ and falls down to zero in a layer of thickness d . It is used as a mask controlling the size of the cancellation support, $\text{supp}(\text{FC})$. We use here the particular values $y_0 = -0.5$, $y_1 = 0.5$, $d = 0.1$, whence $\text{supp}(\text{FC}) \subset \text{supp}(\text{FFF}) \subset \text{supp}(B_z)$ as the width of each Gaussian polarity is approximately equal to 2 and decreases at a slower rate. The case considered in Amari et al. (2000; where FC is enforced over the whole bipolar region) corresponds to $\zeta = 1$. Using Equation (2), we have $\partial_t B_z(x, y, 0, t) = -\mu \zeta(y) q(x, y)$, whence after an immediate integration

$$B_z(x, y, 0, t) = q(x, y)[1 - \mu \zeta(y)(t - t_0)]. \quad (4)$$

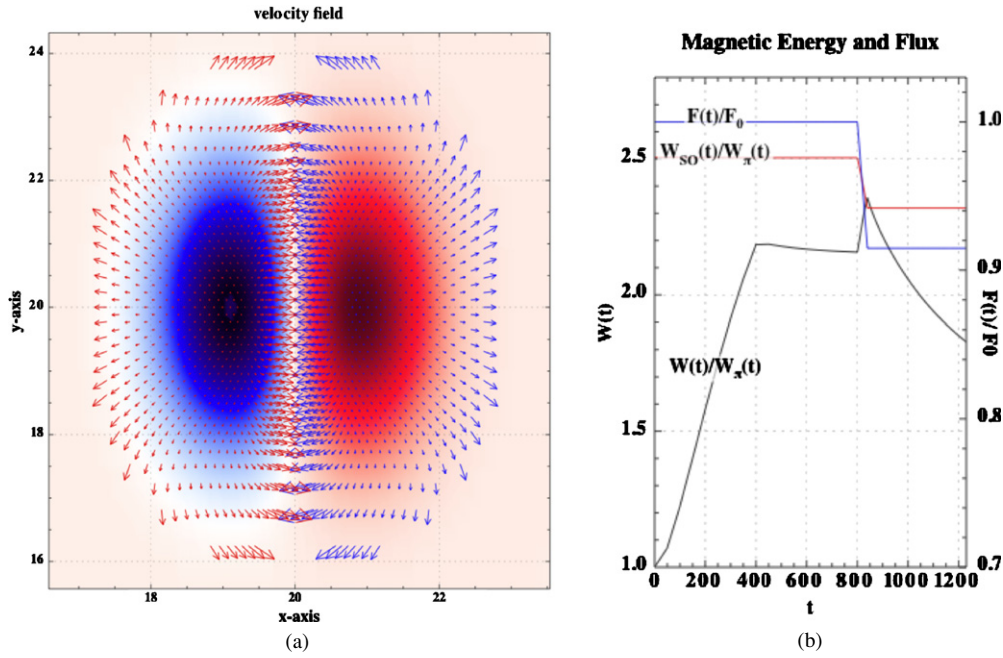


Figure 2. (a) Plot of the velocity field associated with the imposed flux decrease. This flow is indeed a cancellation flow as it brings flux elements of opposite polarities into contact along the inversion line, where they get annihilated. (b) Time variations of some important quantities during the phase of twisting by boundary motions of the initial potential field ($0 \leq t \leq 400$), the phase of viscous relaxation ($400 \leq t \leq 800$), the phase of FC ($800 \leq t \leq 838$), and the NE phase ($838 \leq t$). Represented are the normalized unsigned flux $F(t)/F_0$ through S_h , the free magnetic energy measure $W(t)/W_\pi(t)$ (which increases during the FC phase), and the free energy measure $W_{SO}(t)/W_\pi(t)$ (which decreases during the FC phase) of a semi-open field which has all its open lines originating from the region on which the shear/twist is distributed. The last two curves intersect at some critical time, corresponding to an FC of less than 6%, beyond which the global disruption occurs.

(A color version of this figure is available in the online journal.)

Then B_z suffers a linear decrease on S_h . But this does not lead to any specific problem as the reduction factor $(1 - \mu \zeta(y)(t - t_0)) \geq 0.62 > 0$, the FC phase being limited to a duration of about 38 (see below). All along that phase, we regularly apply viscous relaxation runs to check if a neighboring equilibrium exists or not. We found this strategy to be more appropriate than the one used in Amari et al. (2007), where the need to effect episodic relaxations was bypassed by choosing a much smaller value of μ ($\mu = 10^{-4}$).

As stated in Section 1, it is crucial for the validity of the model that the mathematically imposed flux decrease be interpretable in physical terms. Let us show that it can be actually considered to result from the transport of opposite polarities fluxes toward the inversion line I where they annihilate indeed. In any case, we can introduce on S_h a horizontal velocity of magnetic flux transport, \mathbf{u} , by setting $c \mathbf{E}_s + B_z \mathbf{u} \times \hat{\mathbf{z}} = 0$. Using the Helmholtz decomposition (1) of $c \mathbf{E}_s$ and Equation (4), we obtain at once

$$\mathbf{u}(x, y, t) = -\nabla_s \psi(x, y) / [q(x, y)(1 - \mu \zeta(y)(t - t_0))]. \quad (5)$$

During the FC phase, \mathbf{u} appears to be just continuously rescaled by a time-dependent factor on most of $\text{supp}(\text{FC})$, where $\zeta = 1$, and to remain invariant outside $\text{supp}(\text{FC})$, where $\zeta = 0$. Interestingly, we see that the cancellation flow support, $\text{supp}(\text{CF})$, coincides approximately with $\text{supp}(B_z)$, and is then not reduced to $\text{supp}(\text{FC})$ for a localized FC. The velocity \mathbf{u} computed at some time is shown in Figure 2(a), and it is clearly seen to be directed indeed toward I in a neighborhood of that line. Note that we have removed from the plot the parts very close to I and very far from the spots, respectively, where u becomes very large. The flux $B_z \mathbf{u}$ of B_z keeps, however, a finite value on I , on which $\nabla_s \psi$ does not vanish, and the flow thus continuously advects magnetic flux onto that line, where it disappears. On the other hand, it should be noted that the velocity

pattern at any other time during the FC phase is identical to the one shown in Figure 2(a) because of the simple scaling property proved above.

That flux decrease may be associated with flux annihilation on the inversion line I can also simply be proved in a quite general way as follows. Let us consider for a little while an arbitrary initial distribution $B_z(t_0)$ on S_h and prescribe a flux decrease by setting $\partial_t B_z = f_c(x, y, t)$, with $f_c \leq 0$ on S_h^\pm , where $B_z > 0$ ($f_c \geq 0$ on S_h^- , where $B_z < 0$), and $\int_{S_h} f_c ds = 0$. We define as above the flux transport velocity \mathbf{u} by $B_z \mathbf{u} = c \mathbf{E}_s \times \hat{\mathbf{z}} = \nabla_s \phi \times \hat{\mathbf{z}} - \nabla_s \psi$. Then we have

$$\int_I B_z u_N dl = \int_I (\partial_t \phi - \partial_N \psi) dl = - \int_{S_h} f_c ds > 0, \quad (6)$$

where \mathbf{N} is the exterior normal on S_h to ∂S_h^+ (and then to D), and $u_N = \mathbf{u} \cdot \mathbf{N}$. For estimating the second member, we have used the Gauss theorem, the equation $\nabla_s^2 \psi = f_c$ (which results from Equation (2)), and assumed $\partial_N \psi$ and ϕ to vanish on the far part of the boundary. We can thus conclude that, "in the mean sense," we have in a neighborhood of I (into which \mathbf{N} has been extended) $u_N > 0$ on the + side and $u_N < 0$ on the - side, which corresponds indeed to a finite amount of fluxes of both signs being transported toward I , where they cancel. But of course, for arbitrary functions $B_z(t_0)$ and f_c , and associated sinuous shape of I , we expect to have in general $u_N > 0$ ($u_N < 0$) on the + (-) side of some little part of I , i.e., local emergence of flux, and FC holds only globally. That this does not happen in the particular case considered in this Letter is due to the fact that we consider a configuration with antisymmetric flux distribution ($q(x, -y) = -q(x, y)$, whence $I = \{y = 0\}$), and impose $f_c = -\mu \zeta q$, with ζ symmetric ($\zeta(-y) = \zeta(y)$). Finally, we note the following relation, which holds for the latter

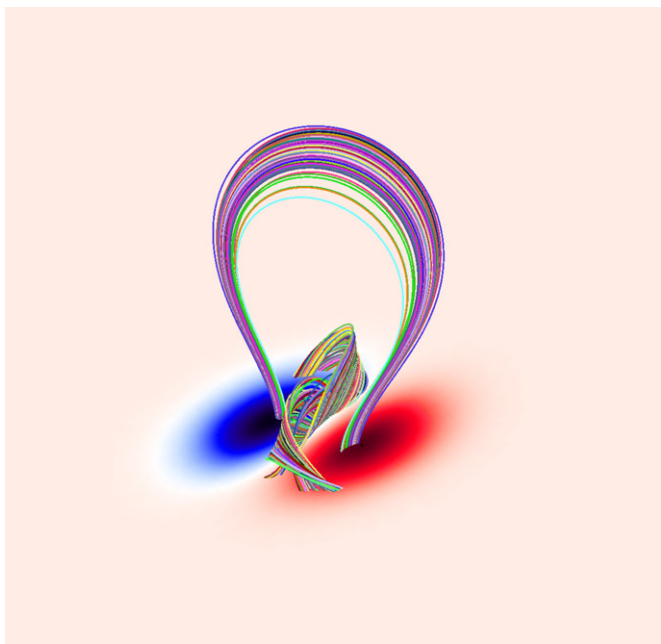


Figure 3. Selected field lines of the equilibrium configuration obtained at $t = 820$, i.e., during the phase of localized FC. A TFR exhibiting dips favorable to the support of cool material has formed from the two J-shape loops shown in Figure 1.

(A color version of this figure is available in the online journal.)

specific choice of f_c . Consider an arbitrary curve C surrounding the positive part of $\text{supp}(\text{FC})$, with external normal $\hat{\mathbf{N}}$. Setting $\Phi(t) = \int_{\text{supp}(\text{FC})^+} B_z ds$ and proceeding as above, we obtain

$$\int_C B_z u_N dl = -d_t \Phi = \mu \int_{\text{supp}(\text{FC})^+} \zeta q ds \simeq \mu \Phi(t_0). \quad (7)$$

Increasing the size of $\text{supp}(\text{FC})$ increases $\Phi(t_0)$ and thus the mean velocity $\langle u_N \rangle$.

For a turbulent diffusion-driven evolution (Amari et al. 2003b), the arguments above, based on our Helmholtz decomposition of \mathbf{E}_s , also apply, thus providing a formal proof that cancellation flows are associated with that process too.

4. TWISTED FLUX ROPE, DISRUPTION, AND TRIGGERING MECHANISM

We now describe the evolution of the coronal field driven by FC.

1. During the first phase, there is a transition from an arcade topology to a TFR topology. This transition is not instantaneous. Rather we observe more and more field lines close to I forming dips and a TFR progressively grows from those as flux is advected toward I . A coherent TFR exists at $t = t_{\text{TFR}}$. In particular J-shape loops have “merged,” generating the inverse topology characteristic of the TFR, with dips able to support prominence material, as shown in Figure 3. Such a feature was also found in the simulations reported in Amari et al. (2000). During the transition, the mutual helicity of the two J-shape loops is converted into the TFR self-helicity.
2. During this phase, viscous relaxation always leads to a neighboring equilibrium. The TFR created along the neutral line grows up both laterally and vertically as new flux participates in its structure. As expected for a system in near equilibrium (Aly 1984, 1991; Sturrock 1991), we find

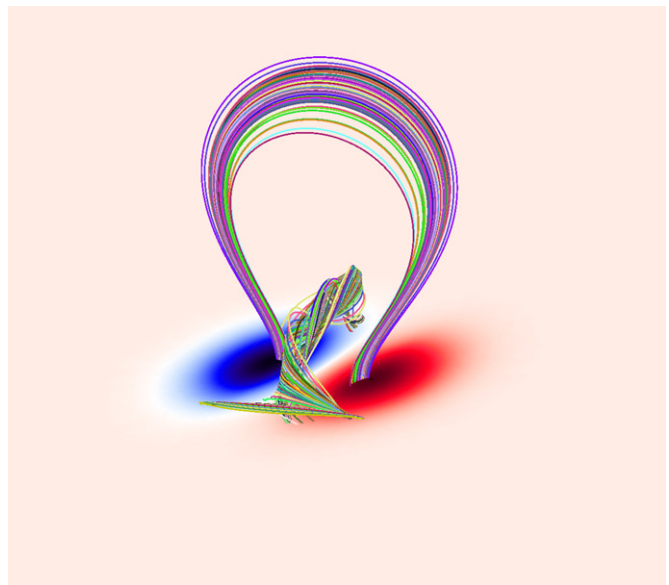


Figure 4. Selected field lines of the evolving configuration at $t = 838$, further during the phase of localized FC. Beyond this state, viscous relaxation to an equilibrium does no longer hold when FC is switched off.

(A color version of this figure is available in the online journal.)

that $W_\pi(t) < W(t) < W_\sigma(t)$, where $W(t)$ is the magnetic energy of the configuration, and $W_\pi(t)$ and $W_\sigma(t)$ are, respectively, the energies of the potential field $\mathbf{B}_\pi(t)$ and the open field $\mathbf{B}_\sigma(t)$ having the same flux distribution on S_h as $\mathbf{B}(t)$. $W(t)$ and $W_\pi(t)$ are observed to decrease slightly, while the ratio $W(t)/W_\pi(t)$ increases (see Figure 2(b)). This behavior is expected since $W_\pi(t)$ depends only on the photospheric flux distribution, decreasing by FC, while $W(t)$ depends also on the volumic distribution of coronal currents. As $W_\pi(t)$, $W_\sigma(t)$ depends only on the photospheric flux distribution and decreases, but the inequality $W_\sigma(t) > W(t)$ stays satisfied as FC has not yet been very effective.

3. After a critical time $t_{gd} \approx 838$, the configuration experiences a global disruption, as shown in Figure 4, and FC is switched off. Viscous relaxation no longer leads to an equilibrium close to $\mathbf{B}(t)$, and the configuration evolves dynamically toward opening (see Figure 5). As in Amari et al. (1996, 2000, 2003a, 2003b, 2007), opening is characterized by a transition to very fast expansion suffered by a bundle of lines, which thus close down eventually at very large distances. Along with that process, reconnection develops through the overlying arcade and a current sheet forms below, associated with dissipation.

At this stage, since our results rely only on viscous relaxation, it can be either that there exists an accessible equilibrium, but that it is unstable (case UE of our classification) or that such an equilibrium does not exist (case NE of our classification). Discriminating between the two situations could be done in principle by first trying to compute force-free equilibria satisfying the boundary conditions on B_n and $\alpha = (\nabla \times \mathbf{B})_z / B_z$ given by the evolution model before and after t_{gd} , respectively (e.g., by using the Grad–Rubin methods developed in Amari et al. 2006), and by studying their stability when they exist. But this is a difficult task since convergence of the equilibrium algorithms might be difficult to achieve around the critical point, while testing stability requires superimposing perturbations of some

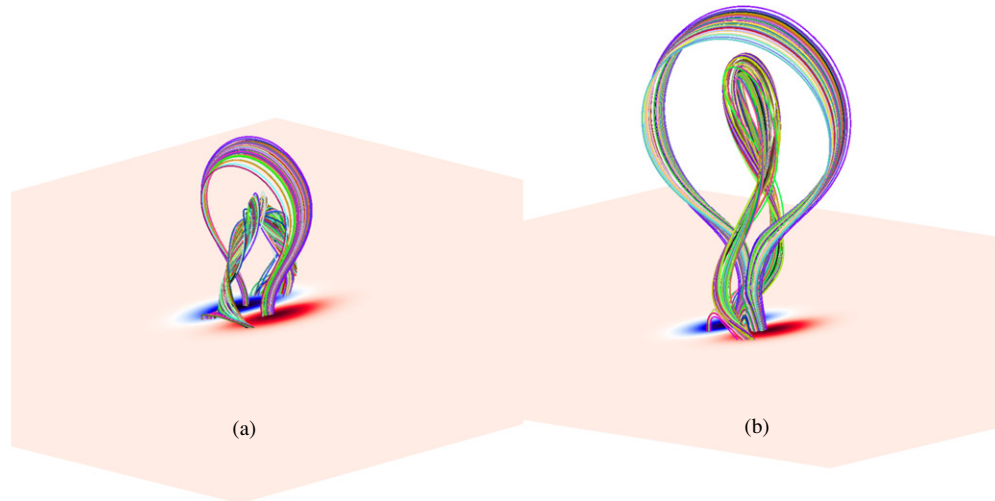


Figure 5. Selection of field lines of the configurations obtained at (a) $t = 885$ and (b) $t = 1135$ from the configuration of Figure 4, with FC switched off. The global disruption involves opening, reconnection through the overlying arcade and below, and formation of a current sheet, associated with a high dissipation of magnetic energy.

(A color version of this figure is available in the online journal.)

types. Then, as we favor a priori NE to be responsible for the disruption, we adopt as in Amari et al. (2000, 2007) the strategy consisting of showing that a necessary condition for the existence of an equilibrium ceases to be satisfied at t_{gd} .

4. The idea is that it becomes energetically favorable for the system to open once the magnetic energy $W(t)$ starts exceeding the energy of an accessible semi-open field $\mathbf{B}_{SO}(t)$. The $\mathbf{B}_{SO}(t)$ which seems to be relevant here is defined as follows: it has all its lines connected to $\text{supp}(\text{SO})$ being open and all the other lines being closed. A priori $\text{supp}(\text{SO})$ can be reasonably defined in two different ways: it can be identified either with the part of S_h to which the fast expanding lines are connected or with the part of S_h where the twist/shear of the initial force-free field is concentrated. Happily, however, the two definitions select the same region $\text{supp}(\text{SO})$. We thus estimate $W_{SO}(t)$ by equating it to the energy of the potential field $\mathbf{B}'_{\pi}(t)$ satisfying $B'_{\pi z} = |q_0|$ on $\text{supp}(\text{SO})$ and $B'_{\pi z} = q_0$ on $S_h \setminus \text{supp}(\text{SO})$. As guessed, it appears that the transition to NE occurs indeed when $W_{SO}(t)$, which decreases faster than $W(t)$, becomes comparable to the latter. In fact Figure 2(b) shows that, while $W(t)/W_{\pi}(t)$ increases, $W_{SO}(t)/W_{\pi}(t)$ decreases, and the two curves cross for $t \simeq t_{gd}$. From this point, any attempt to find a neighboring equilibrium fails and the configuration experiences a major disruption, as shown in Figure 5.

We note finally that the amount of cancelled flux at t_{gd} is about 6%, a small value compared to the 30% found in Amari et al. (2000) and even below the 9% found in the quadrupolar case in Amari et al. (2007). Note that the initial states considered in these previous works were also quite highly sheared. We can thus state that a small amount of FC is sufficient to trigger a large disruption. But we do not pretend in any case that the 6% value is general. Depending on the initial state, a higher or lower amount of partial cancellation may be needed for a large disruption to be produced. And for low shear initial states, it is

even possible that only a confined eruption be obtained as in Amari et al. (2003b).

T.A. thanks G. Aulanier for discussion. We acknowledge support from NASA's Sun-Earth Connection Theory Program, NASA's STEREO/SECCHI Consortium and Centre National d'Etudes Spatiales. The numerical simulations performed in this Letter have been done on the NEC SX8 supercomputer of the Institute I.D.R.I.S of the Centre National de la Recherche Scientifique.

REFERENCES

- Aly, J. J. 1984, *ApJ*, **283**, 349
 Aly, J. J. 1991, *ApJ*, **375**, L61
 Amari, T., & Aly, J. 2009, in IAU Symp. 257, Universal Heliophysical Processes, ed. N. Gopalswamy & D. F. Webb (Cambridge: Cambridge Univ. Press), 211
 Amari, T., Aly, J. J., Mikic, Z., & Linker, J. 2007, *ApJ*, **671**, L189
 Amari, T., Boulmezaoud, T. Z., & Aly, J. J. 2006, *A&A*, **446**, 691
 Amari, T., & Luciani, J. F. 1999, *ApJ*, **515**, L81
 Amari, T., Luciani, J. F., & Aly, J. J. 2005, *ApJ*, **629**, L37
 Amari, T., Luciani, J. F., Aly, J. J., Mikic, Z., & Linker, J. 2003a, *ApJ*, **585**, 1073
 Amari, T., Luciani, J. F., Aly, J. J., Mikic, Z., & Linker, J. 2003b, *ApJ*, **595**, 1231
 Amari, T., Luciani, J. F., Aly, J. J., & Tagger, M. 1996, *ApJ*, **466**, L39
 Amari, T., Luciani, J. F., & Joly, P. 1999, *SIAM J. Sci. Comput.*, **21**, 970
 Amari, T., Luciani, J. F., Mikic, Z., & Linker, J. 2000, *ApJ*, **529**, L49
 Aulanier, G., Török, T., Démoulin, P., & DeLuca, E. E. 2010, *ApJ*, **708**, 314
 Fan, Y. 2001, *ApJ*, **554**, L111
 Forbes, T. G., & Priest, E. R. 1995, *ApJ*, **446**, 377
 Forbes, T. G., et al. 2006, *Space Sci. Rev.*, **123**, 251
 Linker, J. A., Lionello, R., Mikić, Z., & Amari, T. 2001, *J. Geophys. Res.*, **106**, 25165
 López Fuentes, M. C., Demoulin, P., Mandrini, C. H., & van Driel-Gesztelyi, L. 2000, *ApJ*, **544**, 540
 Sturrock, P. A. 1991, *ApJ*, **380**, 655
 van Ballegoijen, A. A., & Martens, P. C. H. 1989, *ApJ*, **343**, 971
 van Ballegoijen, A. A., Priest, E. R., & Mackay, D. H. 2000, *ApJ*, **539**, 983
 Welsch, B. T. 2006, *ApJ*, **638**, 1101
 Yeates, A. R., Attrill, G. D. R., Nandy, D., Mackay, D. H., Martens, P. C. H., & van Ballegoijen, A. A. 2010, *ApJ*, **709**, 1238
 Yeates, A. R., & Mackay, D. H. 2009, *ApJ*, **699**, 1024